KURENAI
Kyoto University Research Information Repository

KYOTO UNIVERSITY

Title	Itinerant electron magnetism of -carbides Co6M6C and Ni6M6C (M=Mo and W)
Author(s)	Waki, T.; Furusawa, D.; Tabata, Y.; Michioka, C.; Yoshimura, K.; Kondo, A.; Kindo, K.; Nakamura, H.
Citation	Journal of Alloys and Compounds (2013), 554: 21-24
Issue Date	2013-03
URL	http://hdl.handle.net/2433/171246
Right	© 2012 Elsevier B.V.
Type	Journal Article
Textversion	author

Kyoto University

Itinerant electron magnetism of η-carbides Co_6M_6C and Ni_6M_6C (M = Mo and W)

T. Waki[a,*], D. Furusawa[a], Y. Tabata[a], C. Michioka[b], K. Yoshimura[b], A. Kondo[c], K. Kindo[c], H. Nakamura[a]

[a]*Department of Materials Science and Engineering, Kyoto University, Kyoto 606-8501, Japan*
[b]*Department of Chemistry, Graduate School of Science, Kyoto University, Kyoto 606-8502, Japan*
[c]*The Institute for Solid State Physics, The University of Tokyo, Kashiwa 277-8581, Japan*

Abstract

Magnetic, transport, and thermal properties of metallic η-carbides Co_6M_6C and Ni_6M_6C (M = Mo and W) with the cubic Ni_6Mo_6C-type structure have been characterized. The Ni-based compounds Ni_6Mo_6C and Ni_6W_6C are Pauli paramagnets with temperature-independent susceptibilities. Susceptibilities of the Co-based compounds Co_6Mo_6C and Co_6W_6C are enhanced and temperature-dependent. Co_6Mo_6C remains paramagnetic down to the lowest temperature, while Co_6W_6C undergoes an antiferromagnetic-type transition at 46 K. A metamagnetic transition was observed for Co_6W_6C at 20–30 T at the lowest temperatures. The correlation among the enhancements in the susceptibility, the resistivity, and the electronic specific heat suggests the presence of moderate electron correlation in these compounds.

Keywords: transition metal alloys and compounds, solid state reaction, electrical transport, heat capacity, magnetisation, high magnetic fields, magnetic measurements

*Corresponding author
Email address:* `waki.takeshi.5c@kyoto-u.ac.jp` (T. Waki)

1. Introduction

Cubic η-carbide-type transition-metal bimetallic compounds T_3M_3X (prototype Fe_3W_3C; denoted as η-6) and T_6M_6X (Ni_6Mo_6C; η-12), where T stands for a $3d$ transition metal, M a $4d$ or $5d$ transition metal in group 4–6, and $X = C$, N, or O, have been studied for about half a century because of their hardness [1, 2] and potential catalytic ability [3]. However their detailed electronic properties remain to be investigated. Recently, a wide variety of magnetic properties of η-6 have been reported by our group [4, 5, 6, 7] and others [8, 9, 10, 11, 12, 13, 14]. For example, we have found that Fe_3Mo_3N show a non-Fermi-liquid behavior at low temperatures [4], and proposed that, in Fe_3Mo_3N, long-range magnetic order is suppressed by the geometric frustration inherent to the η-carbide structure in spite of strong magnetic correlation [5]. Interesting magnetism is also expected in η-12, since η-6 and η-12 are different only in the occupation site of X atoms. In this article, we report briefly low-temperature physical properties of Co- and Ni-based η-12, Co_6Mo_6C, Co_6W_6C, Ni_6Mo_6C, and Ni_6W_6C. The result of an Fe-based η-12, Fe_6W_6C, will be published elsewhere.

2. Experiments

Polycrystalline samples of η-12, Co_6Mo_6C, Co_6W_6C, Ni_6Mo_6C, and Ni_6W_6C, were obtained by solid-state reactions from powdered raw materials. For the Mo-based compounds, a mixture of the $3d$ element, Mo, and C was sealed in an evacuated silica tube and heated in a muffle furnace at 1000°C for 48 h. The synthesis of the W-based compounds was started from a mixture of the $3d$ element, W, and W_2C, and followed by the same procedures. The obtained samples were characterized by X-ray diffraction analysis to have the cubic Ni_6Mo_6C-type structure (space group $Fd\bar{3}m$). Estimated lattice constants at room temperature are 10.903(1), 10.905(1), 10.894(3), and 10.896(2) Å for Co_6Mo_6C, Co_6W_6C, Ni_6Mo_6C, and Ni_6W_6C, respectively; these values are in good agreement with those reported in literatures [15, 16, 17, 18, 19, 20]. Temperature and field dependences of the magnetization in the range from 2 to 300 K and up to 7 T were measured using a SQUID magnetometer, MPMS (Quantum Design), installed at the Research Center for Low Temperature and Materials Sciences, Kyoto University. Temperature dependences of the resistivity were measured for pellets sintered from powder by the four-probe method down to 5 K. Specific heat measurements were performed using a
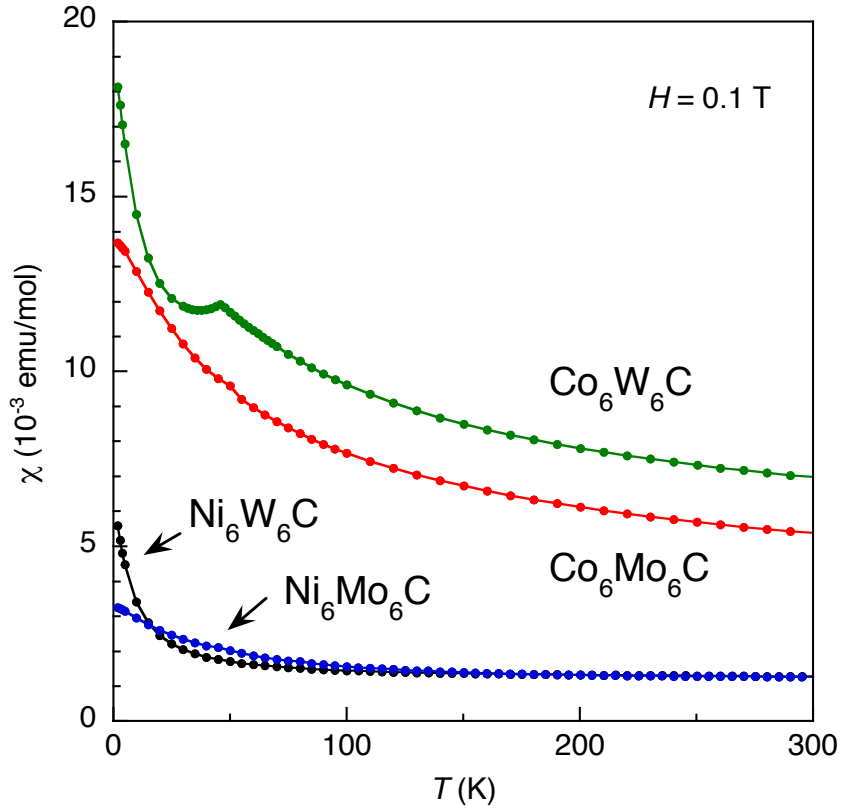
Figure 1: (Color online) Temperature dependences of the susceptibility for η-12.

PPMS (Quantum Design). High-field magnetization measurements up to 54 T were performed with a pulse magnet equipped at ISSP, the University of Tokyo.

3. Results and discussion

3.1. Magnetic susceptibility

Figure 1 shows temperature dependences of the susceptibility $\chi(T)$ for η-12 measured under an external field of 0.1 T. The susceptibility of Co_6Mo_6C has a Curie-Weiss-type temperature dependent term together with a temperature independent contribution. No indication of magnetic order was found down to 2 K. We fitted the data between 100 and 300 K to a modified Curie-Weiss function $\chi(T) = C_C/(T-\theta)+\chi_0$, where C_C is the Curie constant, θ the

3

Table 1: Characteristic values of η-12. A: the coefficient of the T^2 term of the resistivity, γ: the electronic specific heat coefficient, Θ_D: the Debye temperature, GS: the magnetic ground state (AF and P represnt antiferromagnetic and paramagnetic, respectively), and T_N: the Néel temperature.

	$A \times 10^9$ (Ωcm/K^2)	$\gamma \times 10^3$ (J/mol K^2)	Θ_D (K)	GS	T_N (K)
Ni_6W_6C	1.9	37.4	407	P	-
Ni_6Mo_6C	12	82.9	504	P	-
Co_6W_6C	-	87.3	402	AF	46
Co_6Mo_6C	33	113.3	481	P	-

Weiss temperature, and χ_0 a temperature-independent term, and obtained the effective paramagnetic moment $p_\mathrm{eff} = 0.99$ μ_B/Co, $\theta = -73.3$ K, and $\chi_0 = 3.40 \times 10^{-3}$ emu/mol. For the corresponding η-6, Co_3Mo_3C, we have observed a different temperature dependence, namely a broad hump at $\sim$120 K [6], which is characteristic of the exchange-enhanced Pauli paramagnet undergoing an itinerant electron metamagnetic transition. This fact suggests that the C sublattice plays an important role in determining the magnetism.

Co_6W_6C shows a similar temperature dependent susceptibility at high temperatures. The fit of the data between 100 and 300 K to the modified Curie-Weiss function yields $p_\mathrm{eff} = 1.13$ μ_B/Co, $\theta = -93.4$ K, and $\chi_0 = 2.82 \times 10^{-3}$ emu/mol. The obtained values are comparable to those of Co_6Mo_6C, suggesting a similar electronic state at high temperatures. A cusp was observed at $T_\mathrm{N} \simeq 46$ K, indicating the presence of a magnetic transition, probably of antiferromagnetic type.

Susceptibilities for Ni_6Mo_6C and Ni_6W_6C are small and nearly temperature independent, suggesting no significant magnetic enhancement in these compounds. In other words, these compounds are simple Pauli paramagnets. The susceptibility of Ni_6Mo_6C is slightly larger than that of Ni_6Mo_6C except below $\sim$15 K, where Ni_6Mo_6C shows a marked upturn. The low-temperature upturn is probably ascribed to paramagnetic impurities.

3.2. Resistivity

Figure 2 illustrates temperature dependences of the resistivity $\rho(T)$. All the compounds show metallic behaviors with positive temperature coefficients. Residual resistivities $\rho(0)$ are relatively large in the range of 0.05–0.3
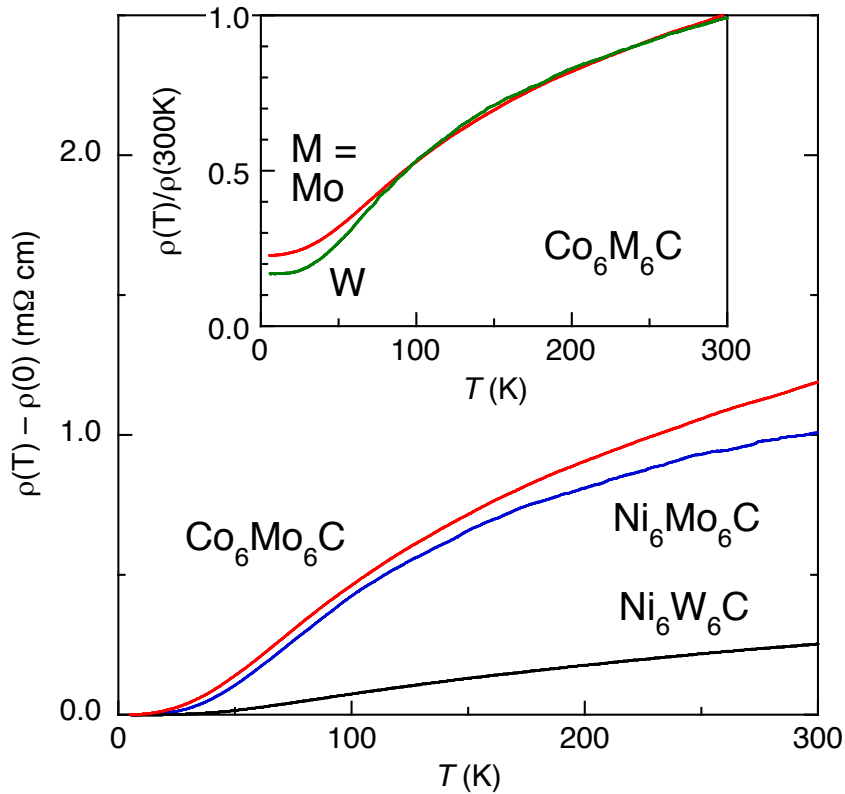
4

Figure 2: (Color online) Temperature dependences of the resistivity for paramagnetic η-12. Residual resistivities were subtracted. In the inset, the resistivity of antiferromagnetic Co_6W_6C, normalized by the value at 300 K, is compared with that of paramagnetic Co_6Mo_6C.

mΩcm because the measurements were performed for sintered pellets, resulting in large errors in the absolute values. The main panel of Fig. 2 shows data of the paramagnetic compounds, where residual resistivities were subtracted to highlight temperature dependences. The temperature variation becomes larger in the order of Ni_6W_6C, Ni_6Mo_6C, and Co_6Mo_6C. At high temperatures, all the curves are not linear but convex upward, suggesting the effect of magnetic fluctuations [21]. At low temperatures, all the three compounds show Fermi-liquid-type quadratic temperature dependences as $\rho(T) = \rho(0) + AT^2$, where A is a coefficient reflecting the electron correlation. Values of A estimated from the data below 15 K are listed in Table 1.

In the inset of Fig. 2, the resistivity of magnetically ordered Co_6W_6C is

plotted and compared with that of the paramagnetic counterpart, Co_6Mo_6C. Here the resistivity was normalized by the value at room temperature. At high temperatures, both the compounds show similar temperature dependences just as in the case of the susceptibility. It is clearly seen that the resistivity of magnetically ordered Co_6W_6C deviates downward in a low-temperature region. Although we have observed no appreciable anomaly just at the expected transition temperature, $T_N = 46$ K, this behavior suggests that the magnetic scattering is reduced associated with the development of magnetic correlation, which is already started from a temperature higher than T_N.

3.3. Specific heat

Figure 3 shows C/T (C: specific heat, T: temperature) plotted against T^2. In contrast to the $-\log T$ divergence observed for Fe_3Mo_3N [4], all present η-12 show Fermi-liquid-type temperature dependences $C/T = \gamma + \beta T^2$, where γ is the electronic specific heat coefficient and β a fitting parameter. Obtained values of γ are listed in Table 1. They are larger than that expected for a simple metal, suggesting moderate electron correlation in these η-12.

The correlation among the enhancements in χ, A, and γ is noticeable for the paramagnetic compounds. According to band calculations for nonmagnetic Co_6W_6C [23], the density of states at the Fermi level $D(E_F)$ is dominated by pronounced Co-3d and relatively broad W-5d components. The Co-3d partial density of states has a peak below the Fermi energy. Based on the rigid band picture, the increase in the number of electrons in the 3d bands results in the reduction of $D(E_F)$. This explains the less magnetic enhancement in the Ni-based compounds. On the other hand, it seems to be difficult to find a reliable argument to explain the M-site dependence of the magnetism.

As seen in the inset of Fig. 3, the specific heat of Co_6W_6C shows a visible anomaly at $T_N = 46$ K in agreement with the $\chi(T)$ data, supporting the occurrence of a magnetic transition. Even in the magnetically ordered state, the low-temperature γ value is comparable to that of non-ordered Co_6Mo_6C, suggesting that most of the spin degree of freedom remains even below T_N.

Debye temperatures Θ_D converted from β using
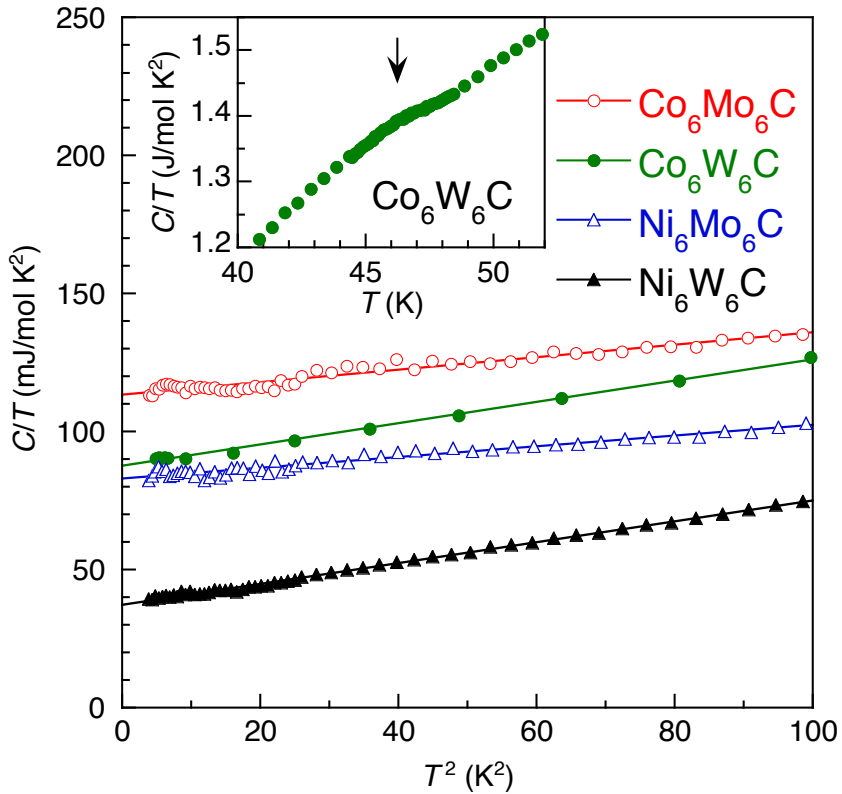
$$\beta = \frac{12}{5}\pi^4 N k_B \Theta_D^{-3}, \tag{1}$$

6

Figure 3: (Color online) C/T vs. T^2 for η-12. The inset is the temperature dependence of C_p/T for antiferromagnetic Co_6W_6C. The arrow represents the temperature where $\chi(T)$ shows an anomaly.

where N is the number of atoms in the system and k_B the Boltzmann constant, are listed in Table 1. The values of Θ_D for the Mo-based η-12 ($\sim$500 K) are comparable to that of WC, 493 K [22]. The W-based η-12 have smaller Θ_D ($\sim$400 K). The fact that the Debye temperature is independent of the $3d$ element but dependent on the M element suggests that the hybridization of $4d$ or $5d$ bands with C $2p$ bands plays an important role in determining mechanical properties.

3.4. High field magnetization

Figure 4 shows field dependences of the magnetization M and its field coefficient dM/dH measured for antiferromagnetic Co_6W_6C at 4.2 K and up to 54 T. The magnetization of paramagnetic Co_6Mo_6C is also included in

the figure for comparison. The magnetization of Co_6Mo_6C is nearly linear in contrast to the η-6 counterpart, Co_3Mo_3C, in which an itinerant electron metamagnetic transition was observed at $\sim$30 T [6]. Generally, the material which shows a hump in $\chi(T)$ shows an itinerant electron metamagnetism and *vice versa* [24, 25]. This trend is confirmed in the present Co-Mo η-6 and η-12 too.

In the field-increasing process, the magnetization of Co_6W_6C increases nearly linearly at low fields and jumps at $H_H \simeq 30$ T. In the field-decreasing process, the magnetization drops at $H_L \simeq 20$ T, resulting in a large hysteresis. The gradient is almost the same below and above the transition, and nearly identical to that of Co_6Mo_6C. In the field increasing process, as seen well in dM/dH, the transition is considerably broadened and, furthermore, looks triggered at around H_L. In other words, there may be two critical fields in the field increasing process.

Temperature dependences of the critical fields, H_H and H_L, are shown in Fig. 5. At low temperatures, H_H and H_L are clearly different, but they tend to merge with increasing temperature and coincide at a temperature of $\sim$30 K much lower than T_N. This fact also suggests that the observation of two critical fields, H_H and H_L, are not due to a simple field hysteresis but to the presence of two phase transitions in the field increasing process, namely the presence of an intermediate phase. Above 30 K, the transition field decreases monotonically to zero at $\sim T_N$. The origin of this characteristic phase diagram remains to be explained, but may be related with the fact that there are two inequivalent Co sites (16d and 32e) in the η-carbide-type structure. Two anomalies in the magnetization process have actually been observed in other η-carbide-type compounds such as Fe_3Mo_3N [5] and Fe_3W_3N [7].

The inset of Fig. 4 shows the Arrott plot (M^2-vs-H/M plot) of Co_6W_6C at 4.2 K. The high-field part is linear, and its intercept at the vertical axis is clearly negative, indicating no intrinsic spin polarization even above the critical field. This fact suggests that the metamagnetic transition is not of the itinerant electron metamagnetism as observed in the η-6 analogue, Co_3Mo_3C, but a change in the magnetic structure, for example, melting of a spin-density-wave (SDW) state to a paramagnetic state or a change in the propagation vector to a different antiferromagnetic state. A similar observation has been reported for a SDW compound, $NbFe_2$ [26].
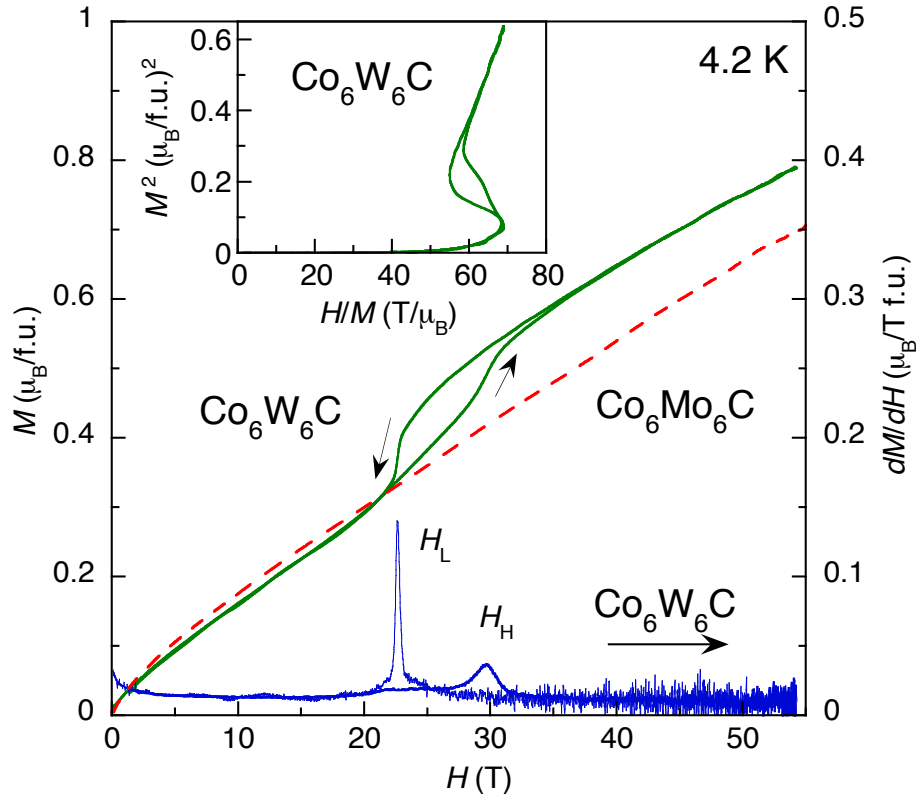
Figure 4: (Color online) Field dependences of the magnetization M and its field coefficient dM/dH of Co_6Mo_6C at 4.2 K. The magnetization curve of Co_6W_6C (broken curve) is also shown. The inset shows the Arrott plot of Co_6W_6C at 4.2 K.

4. Summary

We have measured low-temperature physical properties of Co_6M_6C and Ni_6M_6C (M = Mo and W) with the Ni_6Mo_6C-type structure. Co_6Mo_6C is an enhanced Pauli paramagnet with temperature-dependent susceptibility. Co_6W_6C is an itinerant electron antiferromagnet with $T_N = 46$ K. A metamagnetic transition was also observed at 20–30 T at the lowest temperature. The transition is not of intrinsic spin polarization. Magnetic susceptibilities of Ni_6Mo_6C and Ni_6W_6C are almost temperature independent, indicating that they are Pauli paramagnets.

9
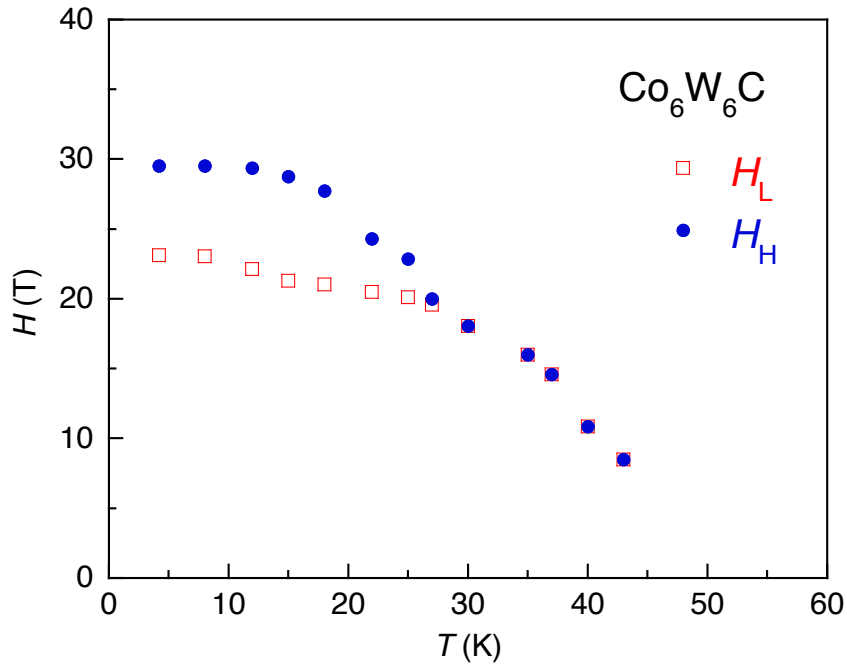
Figure 5: (Color online) Temperature dependences of critical fields for Co_6W_6C.

References

[1] D. Errandonea, Ch. Ferrer-Roca, D. Martínez-Garcia, A. Segura, O. Gomis, A. Muñoz, P. Podríguez-Hernández, J. López-Solano, S. Alconchel, and F. Sapiña, Phys. Rev. B **82** (2010) 174105.

[2] N. A. Dubrovinskaia, L. S. Dubrovinsky, S. K. Saxena, M. Selleby, and B. Sundman, J. Alloys Compd. **285** (1999) 242.

[3] J. J. Pietron, C. Laberty, and K. E. Swider-Lyons, ECS Trans. **3** (2006) 471.

[4] T. Waki, S. Terazawa, Y. Tabata, F. Oba, C. Michioka, K. Yoshimura, S. Ikeda, H. Kobayashi, K. Ohoyama, and H. Nakamura, J. Phys. Soc. Jpn. **79** (2010) 043701.

[5] T. Waki, S. Terazawa, T. Yamazaki, Y. Tabata, K. Sato, A. Kondo, K. Kindo, M. Yokoyama, Y. Takahashi, and H. Nakamura, EPL **94** (2011) 37004.

[6] T. Waki, Y. Umemoto, S. Terazawa, Y. Tabata, A. Kondo, K. Sato, K. Kindo, S. Alconchel, F. Sapiña, and H. Nakamura, J. Phys. Soc. Jpn. **79** (2010) 093703.

[7] T. Waki, S. Terazawa, Y. Tabata, Y. Murase, M. Kato, K. Hirota, S. Ikeda, H. Kobayashi, K. Sato, K. Kindo, and H. Nakamura, J. Alloys Compd. **509** (2011) 9451.

[8] R. N. Panda and N. S. Gajbhiye, J. Alloys Compd. **256** (1997) 102.

[9] S. K. Jackson, R. C. Layland, and H.-C. zur Loye, J. Alloys Compd. **291** (1999) 94.

[10] T. J. Prior and P. D. Battle, J. Mater. Chem. **14** (2004) 3001.

[11] R. N. Panda, G. Balaji, P. K. Pandey, and N. S. Gajbhiye, Hyperfine Interact. **184** (2008) 245.

[12] L. A. Sviridov, P. D. Battle, F. Grandjean, G. J. Long, and T. J. Prior, Inorg. Chem. **49** (2010) 1133.

[13] S. M. Hunter, D. Mckay, R. I. Smith, J. S. J. Hargreaves, and D. H. Gregory, Chem. Mater. **22** (2010) 2898.

[14] P. D. Battle, L. A. Sviridov, R. J. Woolley, F. Grandjean, G. J. Long, C. R. A. Catlow, A. A. Sokol, A. Walsh, and S. M. Woodley, J. Mater. Chem. **22** (2012) 15606.

[15] P. Ettmayer and R. Suchentrunk, Mh. Chem. **101** (1970) 1098.

[16] C. B. Pollock and H. H. Standelmaier, Metall. Trans. **1** (1970) 767.

[17] T. Johannson and B. Uhrenius, Metal Sci. **12** (1978) 83.

[18] V. Ramnath and N. Jayaraman, J. Mater. Sci. Lett. **6** (1987) 1414.

[19] J. M. Newsam, A. J. Jacobson, L. E. McCandlish, and R. S. Polizzotti, J. Solid State Chem. **75** (1988) 296.

[20] N.A. Dubrovinskaia,, L.S. Dubrovinsky, S.K. Saxena, M. Selleby, and B. Sundman, J. Alloys Compd. **285** (1999) 242.

[21] K. Ueda and T. Moriya, J. Phys. Soc. Jpn. **39** (1975) 605.

[22] Y. A. Chang, L. E. Toth, and Y. S. Tyan, Metall. Trans. **2** (1971) 315.

[23] D. V. Suetin, I. R. Shein, and A. L. Ivanovskii, Physica B **404** (2009) 3544.

[24] H. Yamada, Phys. Rev. B **47** (1993) 11211.

[25] Y. Takahashi and T. Sakai, J. Phys.: Condens. Matter **10** (1998) 5373.

[26] Y. Yamada and A. Sakata, J. Phys. Soc. Jpn. **57** (1988) 46.